BMC Medical Imaging

RESEARCH

Open Access

Predictive value of enhanced CT and pathological indicators in lymph node metastasis in patients with gastric cancer based on GEE model

Ling Yang[1†], Yingying Ding[1†], Dafu Zhang[1†], Guangjun Yang[1], Xingxiang Dong[1], Zhiping Zhang[1], Caixia Zhang[1], Wenjie Zhang[2*], Youguo Dai[3*] and Zhenhui Li[1*]

Abstract

Objectives A predictive model was developed based on enhanced computed tomography (CT), laboratory test results, and pathological indicators to achieve the convenient and effective prediction of single lymph node metastasis (LNM) in gastric cancer.

Methods Sixty-six consecutive patients (235 regional lymph nodes) with pathologically confirmed gastric cancer who underwent surgery at our hospital between December 2020 and November 2021 were retrospectively reviewed. They were randomly allocated to training ($n=38$, number of lymph nodes = 119) and validation ($n=28$, number of lymph nodes = 116) datasets. The clinical data, laboratory test results, enhanced CT characteristics, and pathological indicators from gastroscopy-guided needle biopsies were obtained. Multivariable logistic regression with generalised estimation equations (GEEs) was used to develop a predictive model for LNM in gastric cancer. The predictive performance of the model developed using the training and validation datasets was validated using receiver operating characteristic curves.

Results Lymph node enhancement pattern, Ki67 level, and lymph node long-axis diameter were independent predictors of LNM in gastric cancer ($p<0.01$). The GEE-logistic model was associated with LNM ($p=0.001$). The area under the curve and accuracy of the model, with 95% confidence intervals, were 0.944 (0.890–0.998) and 0.897 (0.813–0.952), respectively, in the training dataset and 0.836 (0.751–0.921) and 0.798 (0.699–0.876), respectively, in the validation dataset.

Conclusion The predictive model constructed based on lymph node enhancement pattern, Ki67 level, and lymph node long-axis diameter exhibited good performance in predicting LNM in gastric cancer and should aid the lymph node staging of gastric cancer and clinical decision-making.

Keywords Ki-67 antigen, Lymphatic metastasis, Stomach neoplasms, Gastroscopy, Tomography, X-Ray computed

[†]Ling Yang, Yingying Ding and Dafu Zhang contributed equally to this work.

*Correspondence:
Wenjie Zhang
zxf123hao@163.com
Youguo Dai
daiyouguo@126.com
Zhenhui Li
lizhenhui621@qq.com
Full list of author information is available at the end of the article

Introduction

Gastric cancer is one of the most common malignant tumours of the digestive system. It is the fifth most common type of cancer and third leading cause of cancer-related deaths worldwide [1]. More than 1 million new cases of gastric cancer and approximately 769,000 new deaths were reported in 2020 [2, 3]. The incidence and mortality rates of gastric cancer in China are higher than the global averages, while the survival rate of Chinese gastric cancer patients is below the global level, with the overall 5-year survival being less than 50% [4, 5].

Lymph node metastasis (LNM) is the common route of gastric cancer metastasis, and regional LNM in gastric cancer primarily affects the preoperative staging and extent of surgery. At present, D2 gastrectomy is the standard surgical treatment for advanced gastric cancer, and the detection of at least 16 lymph nodes is required for adequate staging [6–8]. Although D2 gastrectomy is accepted by most researchers as the standard surgical treatment for advanced gastric cancer and is widely applied in clinical practice, discussions regarding the optimal extent of lymph node resection have been ongoing for decades [9, 10]. In early- and advanced-stage gastric cancer, the groups and extents of LNM differ among patients. Therefore, D2 lymph node dissection may not be applicable to all patients (lack of universality), especially in those with early-stage gastric cancer [11]. Excessive lymph node dissection may lead to more postoperative complications and longer postoperative recovery time, while inadequate lymph node dissection may cause stage underestimation and accelerate tumour metastasis. Therefore, the accurate preoperative determination of LNMs in different regions will serve as a strong basis for determining surgical treatment and improving the survival of patients. Enhanced computed tomography (CT) is a routine examination method that is widely used for preoperative lymph node staging in gastric cancer [12].

It is unknown whether generalised estimating equation (GEE)-based logistic regression (GEE-logistic) models that combine preoperative CT indicators and pathological parameters can improve the prediction of LNM in gastric cancer. Hence, this study aimed to establish a tool for the preoperative prediction of LNM in gastric cancer based on simple and reliable imaging and pathological parameters.

Materials and methods

Patients

Sixty-six consecutive patients with gastric cancer who underwent surgery in Yunnan Cancer Hospital between December 2020 and November 2021 were included in this retrospective study. The study was approved by the research ethics committee of the hospital, and the requirement for obtaining a written informed consent was waived because of the retrospective nature of the study. Patients who (1) underwent surgical treatment and were diagnosed with gastric cancer by postoperative pathology, (2) had undergone intraoperative lymph node grouping and harvesting according to the Japanese Classification of Gastric Carcinoma (JCGC), and (3) underwent enhanced CT examination 2 weeks prior to surgery were included in the study. We excluded patients who (1) received preoperative neoadjuvant chemotherapy and targeted therapy, (2) had excessively large respiratory and motion artefacts on CT images, and (3) had other concomitant systemic malignancies. The flowchart of patient selection is presented in Fig. 1.

The clinical and pathological data of all study patients were obtained, including age, sex, body mass index (BMI), tumour site (cardia, gastric body, antrum, pylorus, or two or more tumour sites), T stage, tissue type and differentiation, tumour diameter, Ki67 level, absolute lymphocyte count, absolute neutrophil count, and neutrophil-to-lymphocyte ratio.

CT protocol

Prior to the CT examination, patients fasted for 8–12 h and underwent training to master the breath-hold technique. Fifteen minutes before the examination, 800–1,000 mL of warm water was taken orally, which served as a negative contrast agent. CT examinations were conducted using a Siemens 128-row CT scanner (Definition AS+; Siemens Medical Solutions). Both routine plain CT and enhanced CT were performed with the patients in supine position, from the dome of the diaphragm to the pubic symphysis. The scanning parameters were as follows: tube voltage, 120 kV; tube current, 250 mA; CARE Dose 4D and CARE kV, activated; collimation, 128×0.6; gantry rotation speed, 0.33 s/rot; and pitch, 0.85. Using a double-cylinder high-pressure syringe, the contrast agent iohexol (350 mg I/m; Yangtze River Pharmaceutical Group) was injected into the cubital vein at a flow rate of 3.5 mL/s and dose of 1.5 mL/kg. This was followed by the injection of a 30-mL saline chaser. Arterial and venous phase scans were performed 30 s and 70 s, respectively, after the injection of the contrast agent.

Image analysis

Perigastric lymph nodes were grouped and labelled in accordance with the JCGC [13] by an experienced abdominal radiologist. The groups, order, and sizes of the lymph nodes were recorded and comparatively analysed, and the lymph node groups were determined based on the pathological results. The long- and short-axis diameters, plain CT value, arterial and venous phase CT values

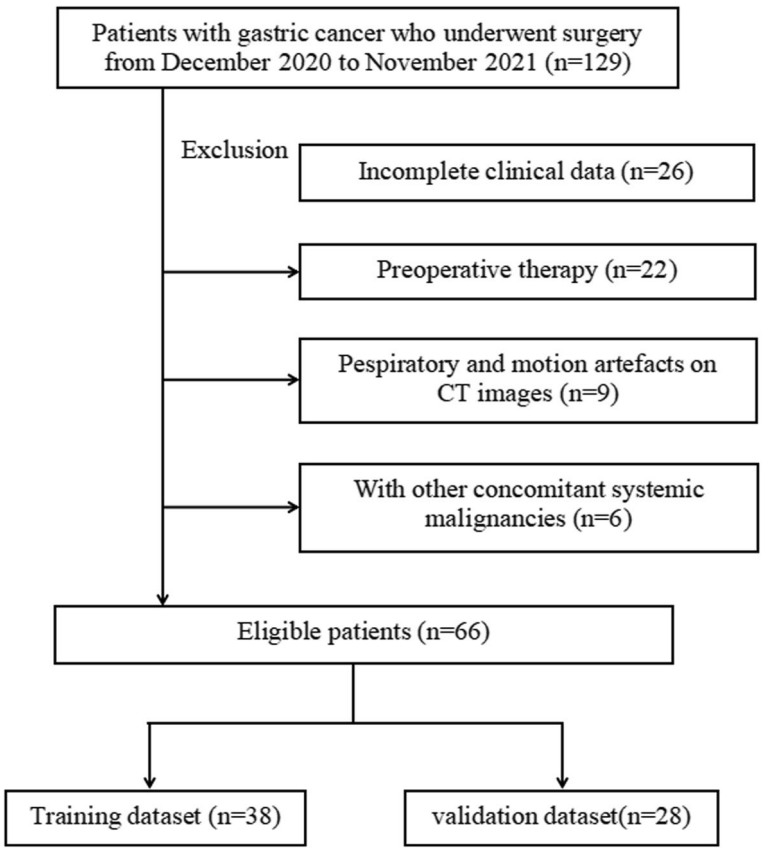

Fig. 1 Flowchart of patient selection

of the lymph nodes, arterial and venous phase CT values of primary gastric cancer lesions, and CT values of the abdominal aorta were measured on the same slices. The long/short diameter ratio, standardised CT values (CT value of lesion/CT value of the abdominal aorta on the same slice) and enhanced arterial/venous phase CT values (arterial/venous phase CT value – plain CT value) were calculated, and the enhancement patterns (homogeneous/inhomogeneous) and morphology (regular/irregular) were observed (Fig. 2). Each lesion was measured thrice, and the mean value of the three measurements was used for the data analysis to reduce measurement errors.

Feature selection and model building

Univariate analysis was used to identify the clinical, imaging, and pathological indicators with statistical significance ($p < 0.05$). The patients were randomly allocated to the training and validation datasets in a 6:4 ratio using computer-generated random numbers. As non-independence may potentially exist among different lymph nodes in the same patient, a forward stepwise logistic regression model based on GEEs (GEE-logistic model) was used [14] for single lymph nodes, and a predictive model for LNM in gastric cancer was constructed using the indicators with statistical significance in the univariate analysis. The GEE-logistic models enabled the distinction at the lymph node level and prevented the amplification of baseline data at the patient level that occurs with standard models [15, 16]. Subsequently, the optimum predictive model was established using regression coefficients and validated using the validation dataset. The receiver operating characteristic (ROC) curves of the model were plotted to calculate the predictive performance of the model.

Statistical analysis

Continuous variables with a normal distribution are expressed as mean ± standard deviation and were compared using the independent two-sample t-test. Continuous variables with a non-normal distribution are expressed as median (interquartile range) and were compared using the Wilcoxon test. The group-specific number and proportion of patients in each category were used to describe the results for categorical data, which were compared using the chi-square (χ^2) test or Fisher's

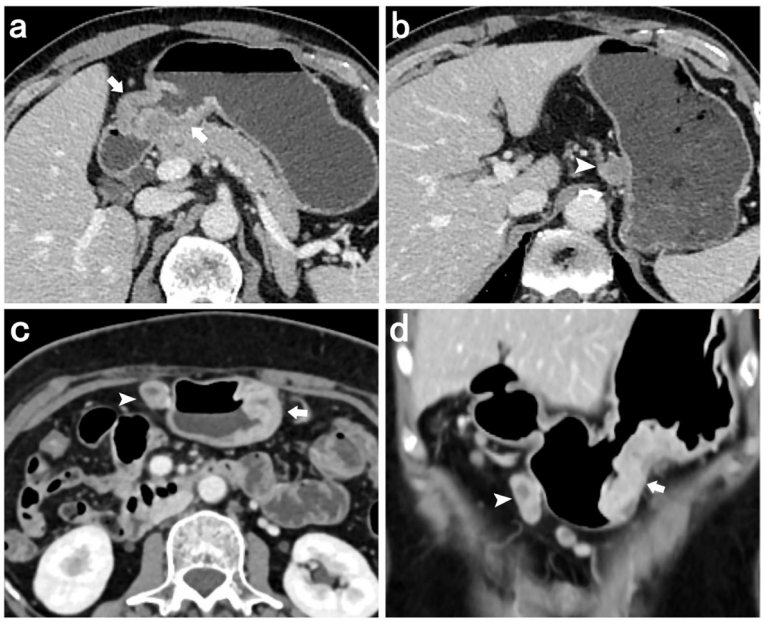

Fig. 2 **a**, **b** Transverse CT image of a 63-year-old male with gastric antrum cancer (**a**, arrow). A contrast-enhanced CT image show lymph node metastasis (**b**, arrowhead) in the stomach lesser curvature with irregular morphology and heterogeneous enhancement. **c**, **d** Transverse (**c**) and coronal (**d**) CT image of a 56-year-old female with gastric body cancer (arrow). Contrast-enhanced CT image show lymph node metastasis (arrowhead) beneath the gastric antrum with regular morphology and heterogeneous enhancement

exact test. A stepwise logistic regression model based on GEE was established to distinguish multiple independent lymph nodes in the same patient. Thereafter, the ROC curves were plotted using the pROC package in R to evaluate the diagnostic performance of the GEE-logistic prediction model among datasets for training, validation, and sensitivity analysis. The area under the curve (AUC), accuracy, sensitivity, and specificity were calculated to assess the predictive ability of the GEE-logistic model. All statistical analyses were performed using R (version 4.1.2, R Foundation for Statistical Computing), all tests were two sided, and a p value of < 0.05 was considered significant.

Results

Clinical characteristics

Sixty-six patients (33 men, 33 women), with a mean age of 54.59 ± 11.50 (range 26–84) years, were included in this study. They were divided into the LNM (38 patients) and non-LNM (28 patients) groups. Univariate analysis revealed significant differences in T stage, Ki67 level, venous phase CT value of gastric cancer lesions, standardised arterial phase CT value of gastric cancer lesions, and standardised venous phase CT value of gastric cancer lesions ($p < 0.05$). However, no significant differences were observed in age, sex, BMI, tumour site, tissue type and differentiation, tumour diameter, absolute lymphocyte count, absolute neutrophil count, neutrophil-to-lymphocyte ratio, and arterial phase CT value of gastric cancer lesions. Table 1 shows the detailed clinical and pathological data of the two groups.

We identified 235 lymph nodes (163 positive LNMs, 72 negative LNMs) in the 66 patients. Results of the univariate analysis showed no significant differences in the standardised venous phase CT values of lymph nodes. However, significant differences were observed in the long-axis diameter, short-axis diameter, enhancement pattern, morphology, venous phase CT value, arterial phase CT value, enhanced arterial phase CT value, enhanced venous phase CT value, standardised arterial phase CT value, and standardised venous phase CT value of the lymph nodes ($p < 0.05$). Table 2 shows the clinical characteristics of the lymph nodes in the gastric cancer patients.

GEE-logistic model building and validation

The patients were randomly allocated to the training and validation datasets using computer-generated random numbers. Variables considered significant in the univariate analysis and long/short diameter ratio were included in the model building process. These included T stage, Ki67 level, venous phase CT value, standardised arterial phase CT value, and standardised venous phase CT value of the primary gastric cancer lesions. Long-axis diameter, short-axis diameter, enhancement pattern, morphology, arterial phase CT value, venous phase CT value,

Table 1 Demographic and clinical characteristics of 66 patients with gastric cancer

Characteristics	Negative LNM ($n=28$)	Positive LNM ($n=38$)	t value/χ^2	*P value*
Age (mean ± sd, year)	51.96 ± 12.99	56.53 ± 10.01	48.94	0.127
Sex			0.062	0.803
Male	15 (53.6%)	18 (47.4%)		
Female	13 (46.4%)	20 (52.6%)		
Location			Fisher[a]	0.518
Cardia	1 (3.6%)	1 (2.6%)		
Gastric body	12 (42.9%)	10 (26.3%)		
Pyloric antrum	13 (46.4%)	22 (57.9%)		
Two or more tumour sites	2 (7.1%)	5 (13.2%)		
T stage			14.422	**0.002**[b]
T1	13 (46.4%)	3 (7.9%)		
T2	5 (17.9%)	7 (18.4%)		
T3	1 (3.6%)	6 (15.8%)		
T4	9 (32.1%)	22 (57.9%)		
Tissue type and differentiation			1.275	0.529
Well differentiated	5 (17.9%)	5 (13.2%)		
Poorly differentiated	22 (78.6%)	29 (76.3%)		
The other tissue types	1 (3.6%)	4 (10.5%)		
Tumor diameter (mean ± sd, cm)	2.30 ± 1.50	3.33 ± 1.94	−2.433	0.018
BMI (mean ± sd, kg/m^2)[c]	22.22 ± 3.55	21.88 ± 2.93	0.389	0.699
Ki67 (mean ± sd, %)[c]	36.25 ± 18.56	49.82 ± 20.57	−2.387	**0.021**[b]
Absolute lymphocyte count (median(IQR),10^9/L)	1.67(1.29, 2.32)	1.63(1.22, 2.02)	Wilcoxon[a]	0.657
Absolute neutrophil count (mean ± sd,10^{12}/L)	3.00 ± 1.05	3.53 ± 1.36	−1.781	0.080
Neutrophil-to-lymphocyte ratio (median(IQR))	0.51 (0.45, 0.74)	0.50 (0.37, 0.78)	Wilcoxon[a]	0.413
Arterial phase CT value of gastric cancer lesions (median(IQR))[c]	86.00 (71.00, 126.50)	96.00 (80.50, 123.80)	Wilcoxon[a]	0.200
Venous phase CT value of gastric cancer lesions (median(IQR))[c]	98.00 (87.00, 112.50)	113.50 (98.25, 132.75)	Wilcoxon[a]	**0.006**[b]
Standardised arterial phase CT value of gastric cancer lesions(median(IQR))[c]	0.21 (0.16, 0.23)	0.25 (0.20, 0.32)	Wilcoxon[a]	**0.020**[b]
Standardised venous phase CT value of gastric cancer lesions (median(IQR))[c]	0.64 (0.58, 0.73)	0.76 (0.66, 0.85)	Wilcoxon[a]	**0.002**[b]

Poorly differentiated includes low differentiate and moderately to low differentiated adenocarcinoma

The other tissue types includes other types of gastric cancer besides adenocarcinoma

BMI Body mass index

[a] Result was analyzed using Fisher's exacted test or Wilcoxon test

[b] Bold values indicate statistically significant numbers

[c] Include some missing values since some patients did not accept these examinations

Well differentiated includes highly differentiated, highly to moderately differentiated and moderately differentiated adenocarcinoma

enhanced arterial phase CT value, enhanced venous phase CT value, standardised arterial phase CT value, and standardised venous phase CT value of the lymph nodes were also included. Eighty-seven lymph nodes from the training dataset (positive LNM, 66 cases; negative LNM, 21 cases) and 89 lymph nodes from the validation dataset (positive LNM, 59 cases; negative LNM, 30 cases) were included in the multivariable model. Results of the multivariate analysis revealed that the lymph node enhancement pattern, Ki67 level, and long/short diameter ratio of lymph nodes were significant (all $p<0.05$) and served as independent predictors of LNM in gastric cancer, with odds ratios (ORs) of 50.522 (95% confidence interval [CI]: 7.8–327.248), 1.068 (95% CI: 1.016–1.121), and 0.129 (95% CI: 0.019–0.85), respectively. For model optimization, the independent variable selection employs a forward stepwise selection method. The GEE-logistic regression model attains its optimal state at Step 12, where it exhibits the smallest QIC value (QIC = 59.53) with an Exchangeable correlation structure. In the resultant optimal multi-factor GEE logistic regression model, only three variables demonstrate statistical significance. Table 3 shows the results obtained from the multivariable GEE-logistic model.

Table 2 Clinical characteristics of 235 lymph nodes in patients with gastric cancer

Characteristics	Negative LNM (*n* = 72)	Positive LNM (*n* = 163)	*t* value/χ^2	*P value*
Long-axis diameter (median(IQR), mm)	8.00 (7.00, 10.00)	9.00 (7.50, 12.00)	Wilcoxon[a]	**0.004**[b]
Short-axis diameter (median(IQR), mm)	5.00 (4.00, 6.00)	6.00 (5.00, 8.00)	Wilcoxon[a]	**0.003**[b]
Long/short diameter ratio	1.50 (1.33, 1.75)	1.50 (1.33, 1.77)	Wilcoxona	0.800
Enhancement pattern			96.184	**< 0.001**[b]
Homogenous enhancement	71 (98.6%)	46 (28.2%)		
Heterogeneous enhancement	1 (1.4%)	117 (71.8%)		
Morphology			18.778	**< 0.001**[b]
regular	67 (93.1%)	106 (65.0%)		
irregular	5 (6.9%)	57 (35.0%)		
Arterial phase CT value of the lymph nodes (median(IQR))[c]	86.00 (71.75, 119.00)	106.00 (81.50, 130.00)	Wilcoxon[a]	**0.009**[b]
Venous phase CT value of the lymph nodes(median(IQR))[c]	92.00 (84.00, 112.50)	103.00 (88.00, 120.00)	Wilcoxon[a]	**0.027**[b]
Enhanced arterial phase CT value of the lymph nodes (median(IQR))[c]	56.50 (40.75, 81.00)	76.00 (50.00, 98.00)	Wilcoxon[a]	**0.011**[b]
Enhanced venous phase CT value of the lymph nodes (median(IQR))[c]	65.50 (52.00, 82.00)	72.00 (61.00, 89.00)	Wilcoxon[a]	**0.020**[b]
Standardised arterial phase CT value of the lymph nodes (median(IQR))[c]	0.21 (0.17, 0.27)	0.26 (0.21, 0.33)	Wilcoxon[a]	**< 0.001**[b]
Standardised venous phase CT value of the lymph nodes (median(IQR))[c]	0.65 (0.58, 0.71)	0.65 (0.60, 0.72)	Wilcoxon[a]	0.612

[a] Result was analyzed using Fisher's exacted test or Wilcoxon test

[b] Bold values indicate statistically significant numbers

[c] Include some missing values since some patients did not accept these examinations

Table 3 Results of the optimal GEE-logistic regression model

Variables	Estimate	SE	Wald χ^2	OR (95%CI)	*p-value*
(Intercept)	−4.073	2.055	15.442	0.017(0,0.955)	**0.047**
Enhancement pattern of the lymph nodes (homogenous vs. heterogeneous)	3.922	0.953	286.686	50.522(7.8,327.248)	**< 0.001**
ki67, %	0.065	0.025	46.612	1.068(1.016,1.121)	**0.009**
Long/short diameter ratio	−2.051	0.964	20.52	0.129(0.019,0.85)	**0.033**

SE standar error, *OR* odds ratio, *CI* confident interval

As shown in Fig. 3, the AUC and predictive accuracy of the model in the training dataset were 0.961 (95% CI: 0.923–0.999) and 92.0%, respectively. The diagnostic sensitivity was 92.4% (5 of 66 positive LNMs were wrongly predicted), while the diagnostic specificity was 90.5% (2 of 21 negative LNMs were wrongly predicted). The negative predictive value was 79.2% (19 of 24 negative LNMs were correctly predicted), while the positive predictive value was 96.8% (61 of 63 positive LNMs were correctly predicted). The AUC and predictive accuracy of the model in the validation dataset were 0.858 (95% CI: 0.781–0.935) and 78.7%, respectively. The diagnostic sensitivity was 67.8% (19 of 59 positive LNMs were wrongly predicted), while the diagnostic specificity was 100.0% (0 of 30 negative LNMs were wrongly predicted). The negative predictive value was 61.2% (30 of 49 negative LNMs were correctly predicted), while the positive predictive value was 100.0% (45 of 45 positive LNMs were correctly predicted).

Discussion

In this study, the predictive model constructed based on the lymph node enhancement pattern, Ki67 level, and long/short diameter ratio of lymph nodes exhibited good performance in predicting LNM in gastric cancer. The model combined CT parameters and pathological indicators to enable better preoperative prediction of single lymph node metastasis.

The criteria for diagnosing perigastric lymph node enlargement and the methods for the preoperative determination of LNM are unclear [17–19]. In recent years, emerging technologies such as dual-energy CT, radiomics, and machine learning have become reliable methods for predicting LNM and the prognosis of gastric cancer [20–22]. Dual-energy CT provides quantitative data (such as iodine value) but requires a slightly higher radiation dose compared with routine enhanced CT. Radiomics and machine learning allow the extraction of more data using big data. Although the resulting models can

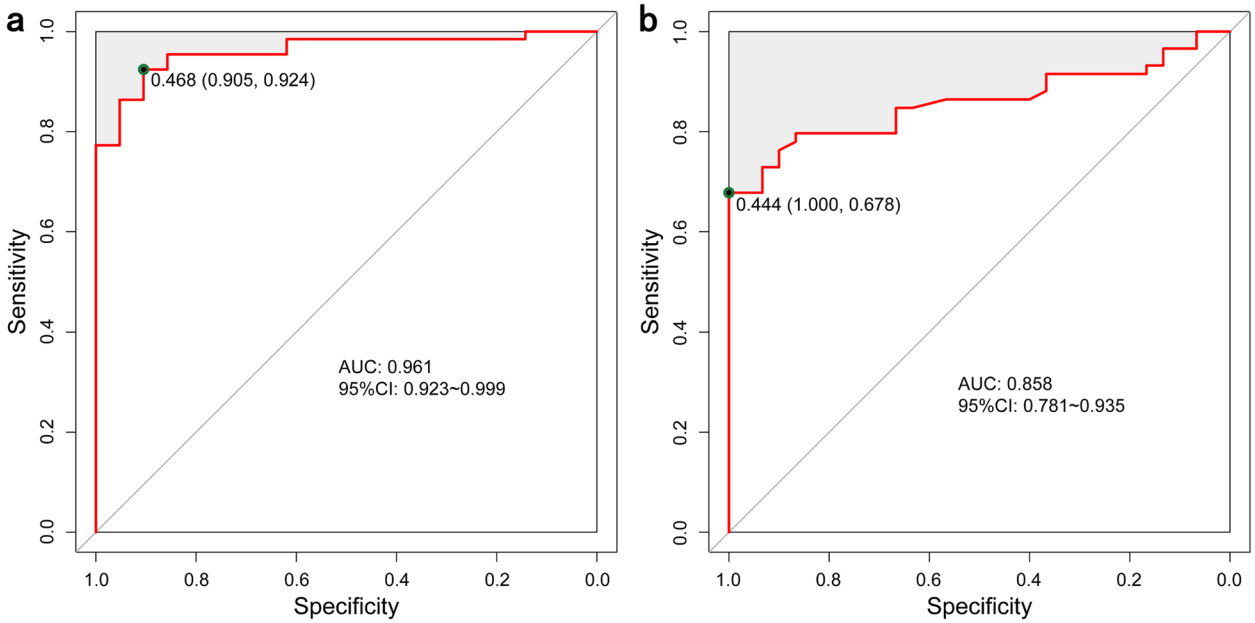

Fig. 3 **a** ROC curves of GEE-logistic model performed in training set (AUC = 0.961). **b** ROC curves of GEE-logistic model performed in validation set (AUC = 0.858). ROC, receiver operating characteristic; AUC, area under the curve; CI: confident interval

achieve better predictive performance, clinical application is difficult due to low repeatability, low generalisability, and the cumbersome data extraction and processing. Studies suggest that the diagnostic and predictive performance of a combination of indicators is superior to that of a single indicator [23]. In the present study, routine enhanced CT indicators were combined with pathological parameters for the construction and internal validation of a predictive model for LNM from gastric cancer. As non-independence may potentially exist among different lymph nodes in the same patient, a forward stepwise logistic regression model based on GEEs was used for single lymph nodes, and a predictive model for LNM in gastric cancer was constructed using the indicators with statistical significance in the univariate analysis. The constructed model included three indicators, namely, lymph node enhancement pattern, Ki67 level, and long/short diameter ratio of lymph nodes. Therefore, the model is relatively simple and utilises parameters that can be easily acquired, which confers high reproducibility in the prediction of LNM.

Lymph nodes are the most abundant type of lymphatic tissue and are widely distributed in the body. When cancer cells migrate to local lymph nodes, they initially grow and proliferate in the outer cortex; this is followed by the gradual involvement of the inner medulla and the entire lymph node. Subsequently, normal tissue structures are replaced with tumour tissues, and swollen lymph nodes may fuse with each other [24]. Tumour cells that have migrated to the lymph nodes are nonuniformly distributed, with the degree of enhancement being generally higher in tumour cell-dense regions and lower in tumour cell-sparse and necrotic regions. This leads to the inhomogeneous enhancement of positive LNMs. Therefore, the enhancement pattern observed in enhanced CT scans can be used to predict LNM. As the degree of enhancement depends on tumour angiogenesis, which occurs at a relatively slow rate, inhomogeneity may be less obvious in smaller lymph nodes. In the present study, 71.8% of the metastatic lymph nodes exhibited inhomogeneous enhancement.

Lymph node size, including the long- and short-axis diameters, is a crucial and the most common indicator of LNM assessed using routine morphology. Previous studies have generally adopted the short-axis diameter as an assessment criterion [25, 26]. However, with the presence of irregular morphology in metastatic lymph nodes, the short-axis diameter may not accurately indicate the lymph node size [27]. In the univariate analysis, no significant differences were observed in long/short diameter ratio of lymph nodes. The requirement for long/short diameter ratio of lymph nodes was included in the multivariate analysis given its clinical significance. In our model, the long/short diameter ratio of lymph nodes was one of the indicators used for the prediction of LNM. The smaller long/short diameter ratio of lymph nodes, the larger the LNM likelihood.

Ki67 can also serve as an indicator for the prediction of LNM. It is an intranuclear protein involved in cell division and proliferation. It is also a marker of proliferative activity. As it is overexpressed in malignant cells and almost undetectable in normal cells, Ki67 is regarded as a valuable marker for prediction and prognostication in gastric cancer [28–30]. The overexpression of Ki67 indicates rapid tumour growth, a low degree of differentiation, and a high degree of malignancy, which increases the tendency of LNM.

The model in the present study has a simple and practical framework. Using the training and validation datasets, the model was able to achieve high AUC values of 0.961 and 0.858, respectively, with high predictive accuracy (92.0% and 78.7%, respectively) and high diagnostic specificity (90.5% and 100.0%, respectively). These results demonstrate the appropriateness and feasibility of parameters used in the constructed model.

The size or T stage of primary gastric cancer lesions are key risk factors for LNM [31, 32]. Results of the univariate analysis indicated that T stage was a significant predictor of LNM, but its predictive potential disappeared in the multivariate analysis. Due to the inherent correlation within lymph node metastases in each case, which constitutes clustered data containing non-independent information, traditional linear models and generalized linear models (e.g., logistic regression, Poisson regression) are unable to effectively process this data, leading to inadequate model fitting. However, GEE provide a suitable method for modeling such clustered or longitudinal data. Designed for simple clustering or repeated measures, GEE is typically applied to non-normal data, including binary and count data. In the present study, the GEE-logistic model was developed for the prediction of metastasis in single lymph nodes to highlight the lymph node characteristics and avoid the elaboration of information related to the primary gastric cancer lesions. Another possible cause of the loss of the predictive power of T stage is the nonuniform T stage distribution among the small sample of patients.

This study has the following limitations: (1) the sample size was small, only internal validation was performed, (2) patient selection bias (only patients that had undergone surgery were included) was observed due to the retrospective nature of the study, and (3) establishing a one-to-one correspondence between a few preoperative positive lymph nodes identified by CT and pathological positive lymph nodes is challenging.

In conclusion, this study is the first to adopt a GEE-logistic method for the construction of a predictive model of LNM from gastric cancer. Our results indicate that this method had good predictive performance. Nonetheless, more data are required for further validation and optimisation of this model.

Abbreviations

AUC	Area under the curve
BMI	Body mass index
CI	Confidence interval
CT	Computed tomography
GEE	Generalised estimating equation
JCGC	Japanese Classification of Gastric Carcinoma
LNM	Lymph node metastasis
ROC	Receiver operating characteristic

Acknowledgements
Not applicable.

Authors' contributions
Ling Yang, Dafu Zhang, Guangjun Yang, Xingxiang Dong, Zhiping zhang, Yingying Ding, Youguo Dai and Zhenhui Li contributed to the study design. Ling Yang, Caixia Zhang and Zhenhui Li performed the scientific literature search, and collated and summarised the identified relevant studies. Ling Yang, Dafu Zhang, Guangjun Yang, Xingxiang Dong, Yingying Ding, Youguo Dai and Zhenhui Li were involved in the data collection. Wenjie Zhang analysed and interpreted the data. Ling Yang and Zhenhui Li wrote the initial draft. The final draft of the report was approved by all authors.

Funding
This study was funded by research grants from the National Natural Science Foundation of China [82001986]; National Science Fund for Distinguished Young Scholars [81925023]; the Applied Basic Research Projects of Yunnan Province, China [202201AY070001-159, 2019FE001-083 and 2018FE001-065]; Yunnan digitalisation, development and application of biotic resource [202002AA100007]; the Outstanding Youth Science Foundation of Yunnan Basic Research Project [202101AW070001]; and the Science Research Fund Project of Yunnan Department of Education [2021J0261].

Data availability
The datasets analyzed in this study are available from the corresponding author on request.

Declarations

Ethics approval and consent to participate
The Third Affiliated Hospital of Kunming Medical University Ethic Committee approval was obtained. The Third Affiliated Hospital of Kunming Medical University Ethic Committee waived the need for written informed consent from the subjects due to the retrospective nature of the study. The study was performed in accordance with the Declaration of Helsinki.

Consent for publication
Not applicable.

Competing interests
The authors declare no competing interests.

Author details
[1]Department of Radiology, the Third Affiliated Hospital of Kunming Medical University, Yunnan Cancer Hospital, Yunnan Cancer Center, Kunming 650118, China. [2]Department of Gastrointestinal Oncology, Harbin Medical University Cancer Hospital, Harbin 150086, China. [3]Department of Gastrointestinal Surgery, the Third Affiliated Hospital of Kunming Medical University, Yunnan Cancer Hospital, Yunnan Cancer Center, Kunming 650118, China.

Received: 14 January 2023 Accepted: 28 January 2025
Published online: 03 February 2025

References

1. Smyth EC, Nilsson M, Grabsch HI, van Grieken NC, Lordick F. Gastric cancer. Lancet. 2020;396:635–48.

2. Sung H, Ferlay J, Siegel RL, et al. Global Cancer Statistics 2020: GLOBOCAN estimates of incidence and mortality worldwide for 36 cancers in 185 countries. CA Cancer J Clin. 2021;71:209–49.
3. Siegel RL, Miller KD, Fuchs HE, Jemal A. Cancer Statistics, 2021. CA Cancer J Clin. 2021;71:7–33.
4. Chen W, Zheng R, Baade PD, et al. Cancer Statistics in China, 2015. CA Cancer J Clin. 2016;66:115–32.
5. Pan R, Zhu M, Yu C, et al. Cancer incidence and mortality: a cohort study in China, 2008–2013. Int J Cancer. 2017;141:1315–23.
6. Japanese Gastric Cancer Association. Japanese Gastric Cancer Treatment Guidelines 2018 (5th Edition). Gastric Cancer. 2021;24:1–21.
7. Egner JR. AJCC Cancer Staging Manual. JAMA. 2010;304:1726–7.
8. Amin MB, Greene FL, Edge SB, et al. The Eighth Edition AJCC Cancer Staging Manual: Continuing to build a bridge from a population-based to a more "personalized" approach to cancer staging. CA Cancer J Clin. 2017;67:93–9.
9. Cuschieri A, Weeden S, Fielding J, et al. Patient survival after D1 and D2 resections for gastric cancer: long-term results of the MRC randomized surgical trial. Surgical Co-operative Group. Br J Cancer. 1999;79:1522–30.
10. Wu CW, Hsiung CA, Lo SS, et al. Nodal dissection for patients with gastric cancer: a randomised controlled trial. Lancet Oncol. 2006;7:309–15.
11. Mogal H, Fields R, Maithel SK, Votanopoulos K. In patients with localized and resectable gastric cancer, what is the optimal extent of lymph node dissection-D1 versus D2 versus D3? Ann Surg Oncol. 2019;26:2912–32.
12. Wang F, Shen L, Li J, et al. The Chinese Society of Clinical Oncology (CSCO): Clinical guidelines for the diagnosis and treatment of gastric cancer. Cancer Commun (Lond). 2019;39:10.
13. Japanese Gastric Cancer Association. Japanese Classification of Gastric Carcinoma: 3rd English edition. Gastric Cancer. 2011;14:101–12.
14. Cao M, Wu T, Zhao J, et al. Focal geometry and characteristics of erosion-prone coronary plaques in vivo angiography and optical coherence tomography study. Front Cardiovasc Med. 2021;8: 709480.
15. Turner EL, Yao L, Li F, Prague M. Properties and pitfalls of weighting as an alternative to multilevel multiple imputation in cluster randomized trials with missing binary outcomes under covariate-dependent missingness. Stat Methods Med Res. 2020;29:1338–53.
16. Paul S, Zhang X. Small sample GEE estimation of regression parameters for longitudinal data. Stat Med. 2014;33:3869–81.
17. Jiang M, Wang X, Shan X, et al. Value of multi-slice spiral computed tomography in the diagnosis of metastatic lymph nodes and n-stage of gastric cancer. J Int Med Res. 2019;47:281–92.
18. Zhong J, Zhao W, Ren F, et al. Lymph node metastasis in patients with gastric cancer: a multi-modality, morphologic and functional imaging study. Am J Transl Res. 2016;8:5601–9.
19. Huang C, Hu C, Zhu J, Zhang W, Huang J, Zhu Z. Establishment of decision rules and risk assessment model for preoperative prediction of lymph node metastasis in gastric cancer. Front Oncol. 2020;10:1068.
20. Dong D, Fang MJ, Tang L, et al. Deep learning radiomic nomogram can predict the number of lymph node metastasis in locally advanced gastric cancer: an international multicenter study. Ann Oncol. 2020;31:912–20.
21. Park CM. Can artificial intelligence fix the reproducibility problem of radiomics? Radiology. 2019;292:374–5.
22. Wang Y, Liu W, Yu Y, et al. CT Radiomics nomogram for the preoperative prediction of lymph node metastasis in gastric cancer. Eur Radiol. 2020;30:976–86.
23. Liu C, Qi L, Feng Q, Sun S, Zhang Y, Liu X. Performance of a machine learning-based decision model to help clinicians decide the extent of lymphadenectomy (D1 Vs. D2) in gastric cancer before surgical resection. Abdom Radiol. 2019;44:3019–29.
24. Vinay K. Robbins basic pathology. 10th ed. Philadelphia: Elsevier US; 2017.
25. D'Elia F, Zingarelli A, Palli D, Grani M. Hydro-dynamic CT preoperative staging of gastric cancer: correlation with pathological findings. A prospective study of 107 cases. Eur Radiol. 2000;10:1877–85.
26. Eisenhauer EA, Therasse P, Bogaerts J, et al. New Response Evaluation Criteria in Solid Tumours: Revised RECIST Guideline (Version 1.1). Eur J Cancer. 2009;45:228–47.
27. Morgagni P, Petrella E, Basile B, et al. Preoperative multidetector-row computed tomography scan staging for lymphatic gastric cancer spread. World J Surg Oncol. 2012;10:197.
28. Luo G, Hu Y, Zhang Z, et al. Clinicopathologic significance and prognostic value of Ki-67 expression in patients with gastric cancer: a meta-analysis. Oncotarget. 2017;8:50273–83.
29. Yang C, Zhang J, Ding M, et al. Ki67 targeted strategies for cancer therapy. Clin Transl Oncol. 2018;20:570–5.
30. Miller I, Min M, Yang C, et al. Ki67 is a graded rather than a binary marker of proliferation versus quiescence. Cell Rep. 2018;24:1105–12.
31. Li J, Fang M, Wang R, et al. Diagnostic accuracy of dual-energy CT-based nomograms to predict lymph node metastasis in gastric cancer. Eur Radiol. 2018;28:5241–9.
32. Chen S, Nie R, OuYang L, et al. Nomogram analysis and external validation to predict the risk of lymph node metastasis in gastric cancer. Oncotarget. 2017;8:11380–8.

Publisher's Note